# A pattern recognition-based horizon auto-tracking algorithm

Yingwei Yu*, Cliff Kelley, and Irina Mardanova, IHS Global, Inc.

Copyright 2013, SBGf - Sociedade Brasileira de Geofísica

This paper was prepared for presentation during the 13th International Congress of the Brazilian Geophysical Society held in Rio de Janeiro, Brazil, August 26-29, 2013.

Contents of this paper were reviewed by the Technical Committee of the 13th International Congress of the Brazilian Geophysical Society and do not necessarily represent any position of the SBGf, its officers or members. Electronic reproduction or storage of any part of this paper for commercial purposes without the written consent of the Brazilian Geophysical Society is prohibited.

**Abstract**

**Horizon auto-tracking could be a very difficult problem at least from two aspects: (1) the selection of pick within a trace usually ignores lateral continuity along dips, and (2) the resulting picks in the same horizon may often conflict with each other in a resulting horizon. In this paper, we proposed a pattern recognition-based algorithm to explicitly address these two difficulties: (1) an array of log-Gabor filters are employed to generate the orientation vectors from seismic amplitude data and guide the pick selection; and (2) a minimum-spanning tree (MST) algorithm can guide and optimize the trace selection to minimize the pick conflictions, which yields a complete and accurate horizon.**

**Introduction**

A horizon is a three dimensional surface defined by seismic reflection events. The goal of the horizon auto-tracking is to track a user selected phase of the horizon curve waveform automatically by a computer program.

The design of the 3D horizon auto-tracking algorithm must deal with the problems of pick selection and trace selection. Pick selection is to find a pick on a given trace. We propose a pick selection method with the aid of orientation vectors calculated for seismic data. Orientation vectors in 3D space can be derived from 2D vectors calculated along the inline and crossline directions. The trace selection is to automatically decide the trace traversal order to apply the pick selection. The trace traversal order is important because the resulting horizon can appear significantly different if the traces are traversed in a different order in the same survey. For example, the resulting horizon generated by line-by-line is quite different to the one by first-in-first-out (FIFO) method. Moreover, the line-by-line approach creates incoherent results for complex horizon. That is, the horizon picks appear very rough and jump across phase cycles from line to line. The same behavior can be observed in a FIFO-based picker.

The pick and trace selection greatly complicate horizon auto-tracking in 3D, and often result in the necessity for experienced interpretors to manually interpret, which is a labor and time intensive process. Our solution is to use orientation vectors to accomplish the above difficulties by guiding pick selection, and optimizing the trace selection by a minimum spanning tree algorithm.

**Method**

In this section, we first introduce the pick selection algorithm using an array of 2D log-Gabor filters to generate orientation vector field (OVF), and then explain how the minimum spanning tree (MST) algorithm is used for the optimized trace selection.

***Pick Selection: Log-Gabor Filter Array***

As observed by Harrigan et al. (1992), horizons generally have a consistently high amplitude reflection signature, and display some degree of lateral continuity. In the practice of horizon tracking, conventional methods usually employ a window-based approach in searching extrema. The window-based approach only looks at the adjacent trace vertically within a time window, while the lateral continuity is ignored. Its very limited context often incurs the "off-cycle" effect where the extrema points are incorrectly linked across seismic phase cycles, which yield a wrong resulting horizon. This effect can be more severe in seismic data with high-angle layering structure.

To preserve the lateral continuity of horizon tracking, we need to examine the seismic data patterns in a range of neighborhoods. The context information reveals which direction the horizon trends. The lateral continuity in 3D can be analyzed by finding horizon curves in 2D vertical slices, in both inline and crossline directions. For each seismic image in 2D, the horizon trends (or the tangent of horizon curves) are the salient continuous features that can be detected visually. Hence filters can be applied to extract the structural features, i.e., the orientation vectors, which preserve the lateral continuity.

In the following, we outline a method of using a bank of optical filters to generate an OVF from a 2D seismic image. The orientation vector is used to post a new pick on each selected trace.

***2D Log-Gabor Filter***

As proposed by Field (1987), natural images have a frequency distribution as Gaussian in logartithmic scale, and the log-Gabor filter has the required logarithmic Gaussian profile. The seismic data follows the rule of natural images. Figure 1 shows the frequency plot of a typical seismic trace. The frequency distribution reflects the logarithmic Gaussian patterns. The 2-D log-Gabor filter is defined in frequency domain as follows (Field, 1987):

$$H(f,\alpha) = H_f \times H\alpha \quad (1)$$

Where $H_f$ is a radial component (see Figure 2a), and $H_\alpha$ is an angular component (see Figure 2b). The radial component is 2D Gaussian in logarithmic scale, and the angular component is Gaussian along orientations.

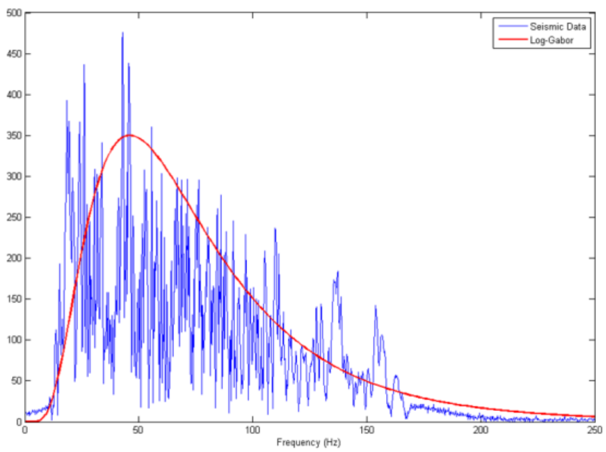


**Figure 1: The Power Spectrum of the Seismic Data Overlay with A Logarithimic Gaussian Curve**. One seismic trace from the experimental seismic data is transformed into frequency domain. The x-axis is frequency and y-axis represents the strength of frequency responses. It shows that the seismic data's spectrum (blue) follows the logarithmic Gaussian distribution (red).

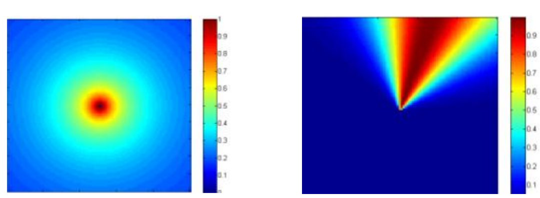

(a) Radial Component (b) Angular Component

**Figure 2: Log-Gabor Filter in Frequency Domain**. (a) Radial component ($H_f$): 2D Gaussian in logarithmic scale. (b) Angular component (Hα: Gaussian along orientations.

***Filter Array***

For input seismic data samples in the spatial domain $I(x,y)$, first apply a Fourier transform into the frequency domain $\hat{I}(u,v)$. The application of log-Gabor filter in frequency domain is,

$$\hat{Y}^{<w,\theta>}(u,v) = H^{<w,\theta>}(u,v)\hat{I}(u,v), \quad (2)$$

where H is the log-Gabor filter with orientation θ and central frequency w. Since it is an array of log-Gabor filters, their central orientations θ can be in a series of orientations, such as $\{-90°, -60°, -30°, 0°, +30°, +60°\}$, and w can be in single or multiple scales as well.

By inverse Fourier transform, we convert $\hat{Y}^{<w,\theta>}(u, v)$ into a complex image in the spatial domain. When we line up all the filter responses for an individual sample at (x, y), we can derive the orientation at this point by getting the location of peak responses in the filter array. In the model, the most salient orientation γ at sample (x, y) is defined by the index of the peak value of the summed orientation responses in all scales *w*:

$$\gamma(x,y) = \mathrm{argmax}_\theta \sum_w \left|Y^{<w,\theta>}(x,y)\right| \quad (3)$$

The γ(x, y) is also referred as the apparent dip (Chopra and Marfurt, 2007). See figure 3(b) for an example, where the dip values are color coded. It is one of the two components of the OVF in the output, the other is the orientation energy E(x, y), which is the sum of filter responses with the orientation γ(x, y) in all scales:

$$E(x,y) = \sum_w \left|Y^{<w,\gamma(x,y)>}(x,y)\right|. \quad (4)$$

The orientation energy E reflects the strength of orientation features. The low values of orientation energy mean that there are fewer oriented patterns in the neighborhood, while the stronger ones mean the orientation feature is more salient in the context. See figure 3(c) for an example.

The same approach can be applied to the OVF calculation in a 3D seismic volume through the combination of inline and crossline volumes. As a result, for each voxel in 3D, we get two vectors one in each of the inline and crossline planes. These vectors serve as a guide for pick selection in 3D data.

***Dip-guided Auto-Tracking***

Given an initial point (or seed point) and the vectors for the initial point in both inline and cross line directions, the pick selection process can be guided by OVF, which contains the following steps:

1. Extrapolating the initial pick onto its neighboring traces by following the orientation vectors.
2. Snapping the extrapolated point to the specific geophysical event (e.g., peaks, trough, or zero-crossing).
3. Extrapolating the initial pick onto its neighboring traces by following the orientation vectors (or the apparent dip angle).
4. Snapping the extrapolated point to the specific geophysical event.
5. Repeating steps 1 and 2 until a stop criteria is matched.

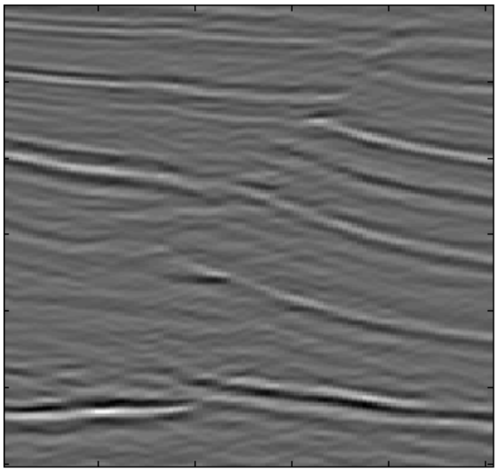

(a) Vertical Seismic Display

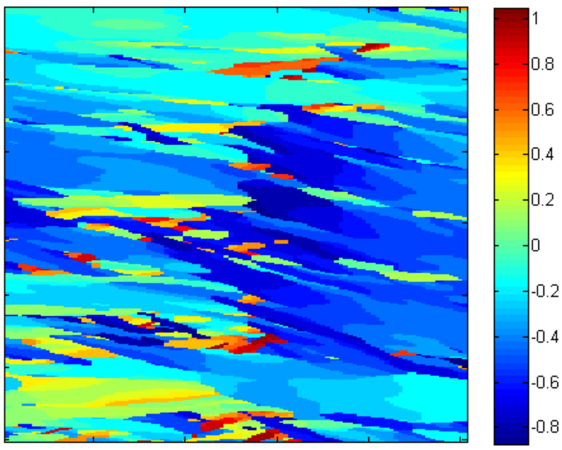


(b) Apparent Dip

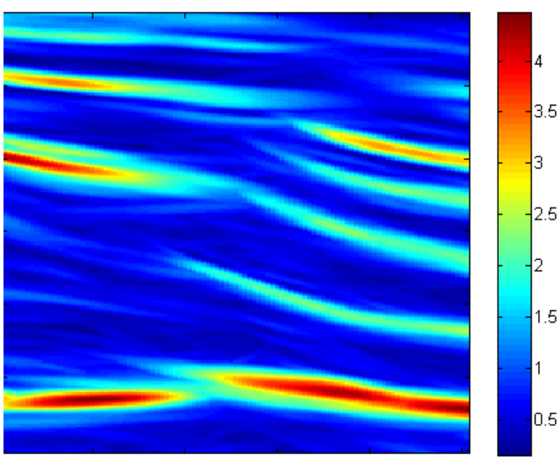


(c) Orientation Energy

**Figure 3: Apparent Dip and Orientation Energy.** (a) a vertical display of seismic slice; (b) the apparent dip derived from (a), and (c) the orientaion energy attribute of (a), which highlight orientation patterns. Seismic data is from the Eagle Ford shale in area of interest.

The pick selection method can be iteratively applied to generate a horizon curve on a 2D seismic slice. However, the pick selection algorithm does not provide a guidance for 3D tracking, and is unable to generate a horizon surface. In the following, we introduce a method on how to traverse the traces within a 3D seismic survey, and show that the traversal order is optimized by maximizing the overall confidence by using an algorithm (MST) from the graph theory.

***Trace Selection: Minimum Spanning Tree***

In our previous work (Yu et al., 2011), we used a minimum spanning tree algorithm to traverse the traces for horizon auto-picking. The idea is to view the trace selection process as a graph traversal problem. A horizon surface can be modeled as an undirected connected graph [N,V], where N is a set of nodes (picks), and V is the set of edges between picks. For example, if pick $p_2$ is derived from a neighbor pick p1, there is an edge drawn between node $p_1$ and $p_2$. If there is a fault between $p_1$ and $p_2$, no edge can be drawn. A spanning tree can then be generated from the root $p_0$ to all the nodes in the graph. A weight, or cost, is then assigned to each edge. The cost is a number defining how unfavorable the edge is. The smaller the cost, the more favorable the edge. The minimum spanning tree (MST) algorithm (Boruvka, 1926; Nesetril et al., 2001) searches through the graph's edges, computes the sum of the costs of the edges, and finds the spanning tree with the minimum cost. The automatic horizon picker in our application employs the MST to find the optimized horizon with the minimum cost and thus the maximum of overall confidence scores.

The MST algorithm applied to horizon auto-picking can be summarized in the following steps (Yu et al., 2011):

1. Start with a collection of initial picks as seeds, which represent the initial current horizon.
2. For the current horizon, apply the pick selection algorithm to extend the picks on the current horizon's boundary in all unfilled directions to their immediate unfilled neighbor traces. Mark these new extended picks as candidate picks, and calculate their confidence values.
3. Select the candidate pick with the maximum confidence among all the candidate picks.
4. Add the candidate pick into the current horizon, and the candidate pick becomes a confirmed pick in the current horizon.
5. Repeat steps 2 to 4 until no new pick can be added. The result is the final horizon.

The confidence value is employed as a heuristic to guide the search for MST, which is calculated based on the patterns of the wavelets around the picks and the locations of the picks. It is bounded between 0 and 1.

## Examples

The described algorithm was tested on 3D seismic survey contains faults and fractures from Eagle Ford shale resource play. To verify the robustness and accuracy of our algorithm, the fault surfaces were not picked prior to the horizon interpretation.

OVF for both inline and crossline planes are calculated before the tracking starts. Each voxel in the seismic data contains two orientation vectors, one along the inline direction, and the other along the crossline direction. Figure 3 shows the apparent dip in (b) and orientation energy in (c) generated in one vertical slice display along inline direction (a).

After generating the orientation vectors, we applied the MST algorithm to search for the horizon picks in 3D. We used only one seed at 2.264 second to pick on the trough event. Figure 4 shows the resulting horizon rendered on a vertical slice (a) and a base map (b). Note that the faults over the horizon are automatically detected by sorting the confidence of candidate picks (see confidence results in Figure 4c), and fault patterns are formed naturally by tracking high confidence picks first in the fault surroundings, leaving the fault area with very low or zero confidence. As shown in the Figure 4a, the horizon segments are correctly picked across several uninterpreted faults with only one seed. These horizon segments appear discontinuous in 2D view; however, they actually connect to each other in 3D. The confidence values are also low at locations around the dome, and is why the picking process stops without going into the dome area.

## Conclusions

In this paper, we proposed a novel method to generate orientation vectors from 3D seismic data. We further applied the orientation vectors in horizon auto-tracking algorithm to guide horizon pick selection. Combining with the MST algorithm in trace selection, one can pick a coherent horizon in 3D seismic data thoroughly and accurately. The proposed horizon auto-picking algorithm can significantly reduce the costs and improve the quality for automatic horizon interpretation. Besides the application in horizon autopicking, the OVF has many potential applications in other seismic interpretation tasks.

## Acknowledgments

The authors would like to thank Global Geophysical Services for providing the seismic data. Thanks to Gary Jones and Rocky Roden for many helpful comments and discussions. This work is protected by US patent 8,265,876.

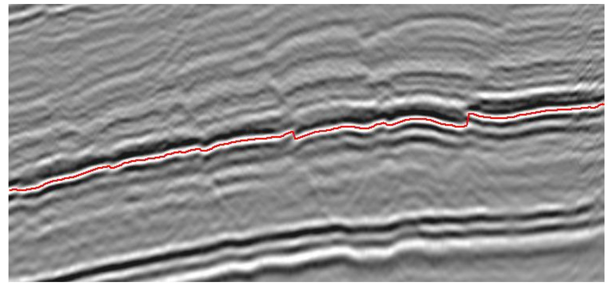

(a) Horizon in Seismic Vertical Slice

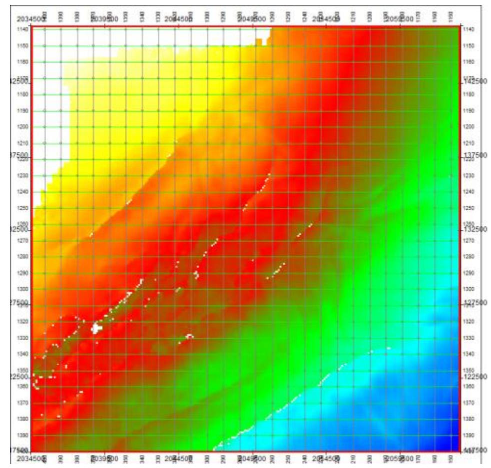

(b) The Resulting Horizon in Base Map View

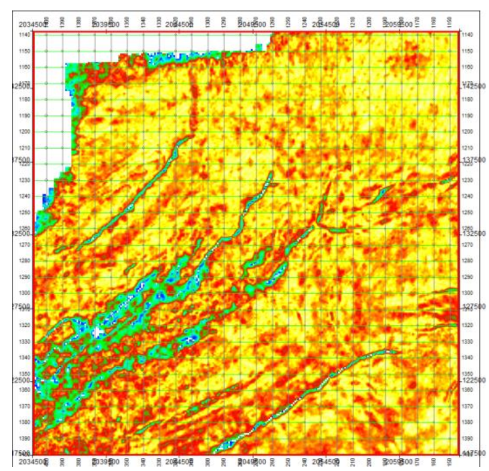

(c) Confidence in Base Map View

**Figure 4: Horizon and its confidence.** (a) In this vertical display, the horizon segments (red) are automatically matched across uninterpreted faults. (b) In the basemap view of horizon, the fault is automatically outlined by picking the points with high confidence in the surrounding. (c) The confidence values are high in flat and clean areas (yellow and red), but low around the faults(cyan and blue). The confidence values are used to prioritize the candidate picks in the queue during the tracking process. Seismic data is from Eagle Ford shale in area of interest, and the horizon is ranged from 2.191 to 2.534 seconds.

**References**

Boruvka, O., 1926, On a certain minimal problem: Praca Moravske Prirodovedecke Spolecnosti (in Czech), 3, 37–58.

Chopra, S., and K. J. Marfurt, 2007, Seismic attributes for prospect identification and reservoir characterization: Society of Exploration Geophysicists.

Faraklioti, M., and M. Petrou, 2004, Horizon picking in 3d seismic data volumes: Machine Vision Application, 15, 216–219.

Field, D. J., 1987, Relations between the statistics of natural images and the response properties of cortical cells: J. Opt. Soc. Am. A, 2379–2394.

Harrigan, E., J. Kroh, W. Sandham, and T. Durrani, 1992, Seismic horizon picking using an artificial neural network: Acoustics, Speech, and Signal Processing, 1992. ICASSP-92., IEEE, 3, 105-108.

Nesetril, J., E. Milkova, and H. Nesetrilova, 2001, Otakar boruvka on minimum spanning tree problem: Translation of both the 1926 papers, comments, history: DMATH: Discrete Mathematics, 233.

Yu, Y., C. Kelley, and I. Mardanova, 2011, Automatic horizon picking in 3D seismic data using optical filters and minimum spanning tree: 81st Annual International Meeting of Society of Exploration Geophysicists, SEG Expanded Abstracts, Society of Exploration Geophysicists, 965–958.